MODELING OF CASTING, WELDING AND ADVANCED SOLIDIFICATION PROCESSES

VII

Proceedings of the seventh conference in a series on modeling casting and welding processes held in London, England from 10-15 September 1995.

Edited by

Mark Cross
Centre for Numerical Modelling and Process Analysis
University of Greenwich
London, UK

John Campbell
School of Metallurgy and Materials
University of Birmingham
Birmingham, UK

A Publication of
TMS
Minerals • Metals • Materials

nal Metals Reviews, pages 75–115, 1976.

in aluminium DC casting caused by exuda-
36(18):4335–4340, 1993.

. and O. R. Myhr. Modelling the surface
ciler, editor, *Light Metals*, pages 889–896,

tallforschung, 2:69–75, 1947.

ory of inverse segregation. *Trans. AIME*,

Part I. *Transactions of the Metallurgical*

ectionally solidified Al-Cu-Ti alloys with
87, 1985.

tion in the mushy zone during solidification
, 24A:963–973, 1993.

n Strangguß. *Metall*, 31(2):163–170, 1977.

ienseigrungen beim NE-Strangguß. *Metall*,

ct of casting speed and metal level on the
ndale, PA, USA, 1993. TMS-AIME.

pper alloy directionally cast with exudation
71.

ear a cast surface caused by exudation and
e *International Journal of Heat and Mass*

sothermal coarsening of dendritic equiaxial
ngineering, A148:289–297, 1991.

Metallurgical Transactions, 22A:569–574,

ase model for transport phenomena during
1, 1991.

The Grain Structure of Castings:

Some Aspects of Modelling

A. Hellawell, Metallurgy and Materials Engineering,

Michigan Technological University, Houghton, MI 49931

Abstract

The efficacy of the modelling of the solidification of castings is typically tested against observed cooling curves and the final grain structures and sizes. Without thermo-solutal convection, equiaxed grain formation is promoted by introduction of heterogeneous substrates into the melt, as grain refiners. With efficient thermo solutal convection, dendrite fragments from the mushy zone can act as an intrinsic source of equiaxed grains and resort to grain refining additions is unnecessary. The mechanisms of dendrite fragmentation and transport of these fragments are briefly considered.

Modelling of Casting, Welding and Advanced SolidificationProcesses VII
Edited by M. Cross and J. Campbell
The Minerals, Metals & Materials Society, 1995

INTRODUCTION

It is taken to be axiomatic that it is desirable to be able to predict the microstructure of a fabricated material shape, to be able to use this information to predict optimal mechanical or physical properties and, at the same time, to identify the best processing path. To be able to do this with confidence must be regarded as enormously, intellectually satisfying and it obviously has vast economic potential for industrial practice. In the metallurgical industry, casting and processing by solidification is (still) the major path for producing final shapes or material suitable for subsequent mechanical working, so the challenge is, to be able to predict the grain structures and grain sizes which evolve at this stage.

The microstructure is determined by nucleation and growth, sometimes taking place concurrently, and the rates at which these occur are determined by the rate of heat removal, primarily of the latent heat. Experimentally, with an opaque material, a metal, the most direct measurement that can be made of the course of the solidification reaction is that of latent heat evolution, followed by a cooling curve, coupled, of course, by examination of the final grain structure. Any models which are developed to describe the overall process must be able to predict the cooling curve at any position in a casting and the accuracy of this curve fitting, coupled with that of the predicted structure and grain sizes is the measure of success. We are still at the stage of testing models, back calculating from actual cooling curves to adjust the computational procedures to yield the correct result and in many cases (eg. 1-3) the results are impressive. However to be truly predictive, from first principles, if indeed that ever becomes possible, we shall need to get the physics right and it seems appropriate to examine some aspects of this many sided problem, with that in mind.

MODELLING PROCEDURES

The latent heat evolution is a consequence of growth, but the distances over which this takes place are determined by the separation between nucleation points. In the following, attention will focus on the origin of these nucleation events, which determine the final grain size in the equiaxed region of a casting. Ideally, the preferred structure would be one of fine, randomly oriented, crystal grains. Long, textured, columnar grains, with attendant problems of macrosegregation and centreline connections are to be avoided. The heat flow analysis, although involved, is now somewhat routine, and is performed by linking finite elements of "suitable" size, having linear gradients within each element. Thermal analysis results also relate to finite elements, which, although cooling or locally heating, as during recalescence, are regarded as being spatially isothermal, and, by implication, of dimensions less than $\sqrt{\kappa t}$ (thermal diffusivity, κ, and relevant time interval, t). For a liquid metal ($\kappa \approx 10^{-5} m^2 s^{-1}$), with a tracking time interval of $t \approx 10^{-2}$s, this implies a finite element of $\lesssim$ 300μm, which may be smaller than the separation of actual nucleation events. On a statistical basis, these physically inconsistent facets of the computational procedure can probably be overlooked and in the following, it is assumed simply, that the local rate of heat removal is constant, or can be calculated, which is acceptable in a low temperature gradient environment. The procedure then follows that originally demonstrated by Oldfield (4) for the nucleation and radial growth of eutectic cast iron grains or "cells". In this, Oldfield simply assumed a given nucleation rate, without seeking to define the physical origin of the nuclei, implicitly assuming that they were some sort of heterogeneous sites (possibly intrinsic iron or graphite fragments) which became active at small undercoolings. The number of these could be predicted with confidence because the "cell" sizes for given cooling rates are very well documented in cast irons. In general, however, the source(s) of nuclei and their activity(ies) vs undercoolings are not well known, and this is of concern here. Either, grains nucleate on heterogeneous substrates

.o predict the microstructure of a fab-
on to predict optimal mechanical or
.e best processing path. To be able to
', intellectually satisfying and it obvi-
e. In the metallurgical industry, cast-
r path for producing final shapes or
.o the challenge is, to be able to pre-
this stage.

wth, sometimes taking place concur-
d by the rate of heat removal, prima-
e material, a metal, the most direct
ification reaction is that of latent heat
rse, by examination of the final grain
: the overall process must be able to
nd the accuracy of this curve fitting,
ves is the measure of success. We are
n actual cooling curves to adjust the
d in many cases (eg. 1-3) the results
first principles, if indeed that ever
and it seems appropriate to examine
ind.

URES

ıt the distances over which this takes
on points. In the following, attention
h determine the final grain size in the
:ture would be one of fine, randomly
s, with attendant problems of macro-
ed. The heat flow analysis, although
' linking finite elements of "suitable"
ermal analysis results also relate to
eating, as during recalescence, are
:ation, of dimensions less than $\sqrt{\kappa t}$
r a liquid metal ($\kappa \approx 10^{-5} m^2 s^{-1}$), with
element of $\lesssim$ 300μm, which may be
)n a statistical basis, these physically
probably be overlooked and in the
ıt removal is constant, or can be cal-
:nt environment. The procedure then
the nucleation and radial growth of
ply assumed a given nucleation rate,
:i, implicitly assuming that they were
iron or graphite fragments) which
these could be predicted with confi-
: very well documented in cast irons.
ctivity(ies) vs undercoolings are not
ıucleate on heterogeneous substrates

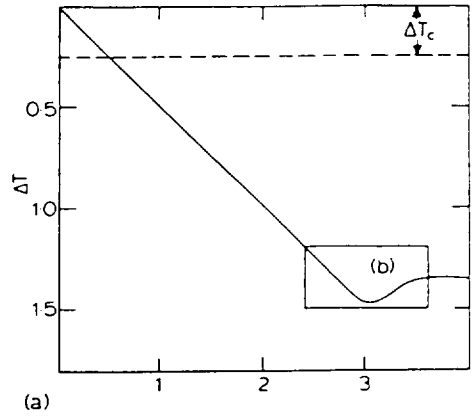

Fig.1(a) Initial part of cooling curve, computed for time dependent nucleation of aluminium on a substrate dispersion (nominally of Al_3T_1, with $\theta = 7^o$) of particle density, $N^P/v = 10^3 mm^{-3}$ and radii, r = 1μm.

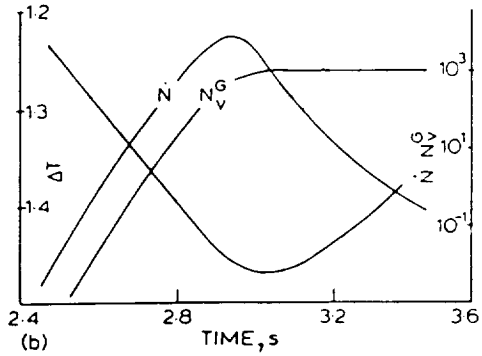

Fig. 1(b) Enlarged region for recalescence, showing superimposed nucleation rate, N, and sum of nucleation events to give a final grain size, N^G/v.

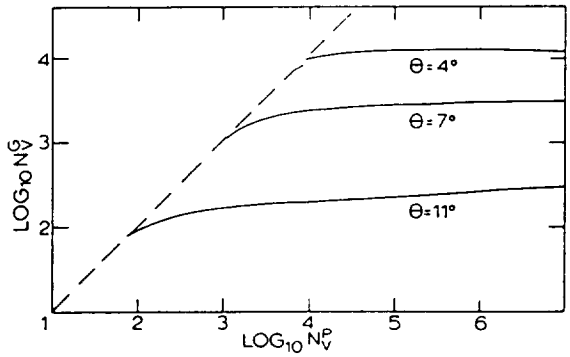

Fig.2 Logarithmic plot of N^G/v (grain size) vs substrate particle density, N^P/v, assuming only one nucleation event per particle, showing excess of substrates for different assumed contact angles, θ. Refer to Fig. 1 for $\theta = 7^o$.

which are deliberately introduced to the melt, as grain refining additions, as in aluminium base castings (eg. 5,6), or, in the absence of such identifiable sources, the most probable origins are taken to be particles of the base material, intrinsically present in the system as crystal fragments, especially, in larger castings, dendritic fragments from an earlier developing mushy region.

In the first case, the nucleation occurs only while the temperature is falling and a little after the recalescence has taken place, the grain size is determined at this very early stage and there may remain a considerable excess of particles which did not have an opportunity to act as substrates. Figs. 1 and 2, summarize this situation (7), although the action of the substrates remains obscure and difficult to quantify (eg. 6-10).

In the second case, with a dispersion of surviving primary fragments, there is no nucleation in the classical sense and the recalescence is entirely described by growth. It follows, that all the surviving crystal fragments grow into grains and there is no residue. If, as it is generally assumed and is well documented (eg. 11-16), these fragments originate from within a preceeding columnar mushy zone, it is necessary to address the problem of (i) how do the fragments develop within the mushy zone and (ii), how are they transported from the mushy region into the bulk liquid? These two aspects of the intrinsic model will be considered here.

DENDRITE FRAGMENTATION

In a casting, following the evolution of a columnar front from an initial chill zone, the dendritic growth proceeds as a well oriented array (<l00> in cubic metals), with the *growth rate decreasing* (approximately, parabolically) and the *temperature gradient falling* as the thickness of the casting develops. The growth conditions are therefore always transient.

The geometry of the growth, Fig. 3, is described by a primary interdendritic spacing, λ_1, measured across a square grid section and a primary dendrite tip radius, r_1, both dimensions determined by the growth rate and temperature gradient, leading to an undercooling, ΔT, at the growth front, for a given concentration in a given system (eg. 17, 18). The undercooling is almost entirely produced by solute build up, ΔC, and the curvature undercooling is negligible. A stable, steady state solution to these dimensions is preferred.

Behind the growth front, secondary dendrite side arms develope with a nascent spacing, λ_2^o, which, for a given material, is in an approximately constant ratio to r_1 (19). For example, in NH_4Cl-H_2O, the ratio is ≈ 4X. Ripening of the side arms begins, almost at once, to give a coarser secondary spacing, λ_2^t, according, approximately, to a relationship of the form $(\lambda_2^t)^3 - (\lambda_2^o)^3 = C_1 t$ (eg. 20), where C_1 is a constant and t = time.

Under steady state conditions, without interdendritic fluid flow, Fig. 4, the ripening assembly shows that surviving side arms typically develope a narrow neck, where they join the primary stems, but remarkably few, if any, actually become detached. This observation is, at first sight, perplexing, because the evidence is that very large numbers of dendrite fragments can be seen to escape from the mushy region of a casting (eg. 21). It is therefore necessary to address this contradiction.

The immediate reaction, knowing that there can be (see next section) vigorous reentrainment and circulation of bulk liquid into the mushy region, is to suppose that this is the cause of enhanced side arm detachment, either by mechanical deformation at the narrow necked positions, or by accelerated melting, because the bulk liquid is warmer (positive temperature gra-

ıing additions, as in aluminium
sources, the most probable ori-
ly present in the system as crys-
ents from an earlier developing

ature is falling and a little after
ıed at this very early stage and
d not have an opportunity to act
ɔugh the action of the substrates

agments, there is no nucleation
ɔd by growth. It follows, that all
no residue. If, as it is generally
ıts originate from within a pre-
problem of (i) how do the frag-
ɔy transported from the mushy
model will be considered here.

)N

m an initial chill zone, the den-
ic metals), with the *growth rate*
re gradient falling as the thick-
fore always transient.

ıary interdendritic spacing, λ_1,
: tip radius, r_1, both dimensions
ding to an undercooling, ΔT, at
(eg. 17, 18). The undercooling is
-vature undercooling is negligi-
ɛrred.

ope with a nascent spacing, λ_2^o,
ratio to r_1 (19). For example, in
ɛgins, almost at once, to give a
a relationship of the form $(\lambda_2^t)^3$

w, Fig. 4, the ripening assembly
neck, where they join the pri-
ɛtached. This observation is, at
numbers of dendrite fragments
21). It is therefore necessary to

section) vigorous reentrainment
uppose that this is the cause of
ıtion at the narrow necked posi-
ırmer (positive temperature gra-

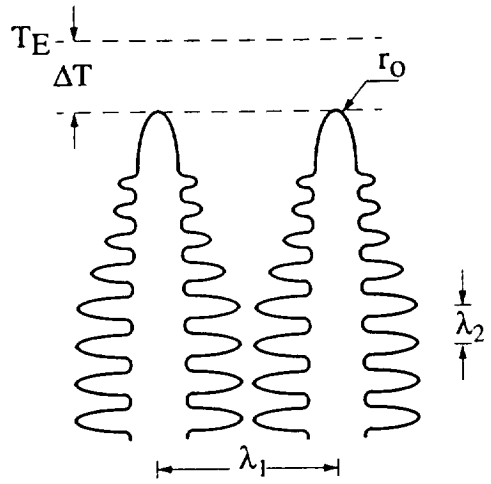

Fig. 3 Schematic dendritic growth front to show relevant dimensions which are referred to in text.

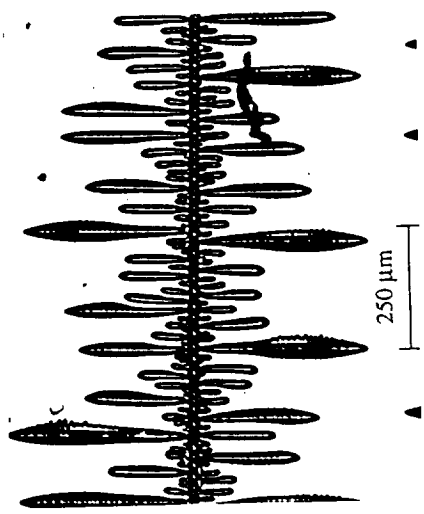

Fig. 4 Dendrite growth in NH_4Cl-H_20 at 20µms^{-1} under steady state conditions - without side arm detachment.

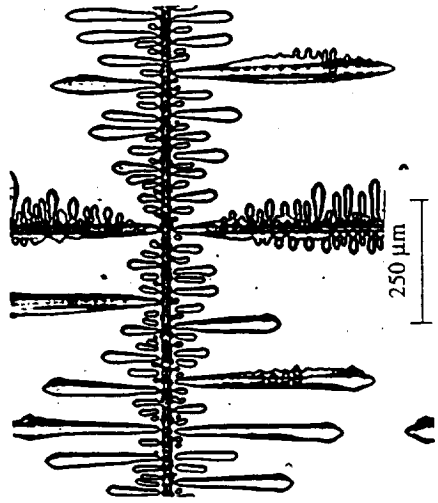

Fig. 5 Similar region, growth at same rate, but followed by deceleration to 8µms^{-1} - showing extensive detachment of side arms.

dient).

Of these two possible mechanisms, the first can probably be discounted, certainly for metals, because at the melting point, the material is so ductile that arms could only bend, but not fracture. We have no evidence of bent side arms.

The second possibility, that melting off is caused by entrainment of the warmer liquid, is more attractive, until it is remembered that the bulk liquid is also less concentrated than the interdendritic liquid, i.e., it is *solvent* rich, so that as it cools, solid will be deposited (preferentially into the flow direction) and melting will not be accelerated. This then is not an obvious cause of the side arms becoming detached.

The solution to this problem must lie in the fact that all real growth conditions are transient - as noted, with growth rate, V and temperature gradient, G, falling continuously. It is necessary to examine how the growth front, and the region behind it, respond to these changes. Observation shows, Fig. 5, that with a step reduction in growth rate, without convection, a majority of side arms become detached - almost at once. Jackson et al. showed this effect nearly twenty years ago (12), although they did not pursue it further at that time.

The observation then is, that at the growth front, the radius of curvature, r_1, responds immediately to change in growth rate, increasing as velocity decreases, according to Vr_1^2 = constant. In contrast, however, the primary spacing, λ_1, does not change rapidly, because it is constrained by the orthogonal restrictions which are created by the small anisotropy of the interfacial energy. λ_1 does not increase immediately, with r_1, nor, with acceleration, does it decrease rapidly. To increase λ_1, it is first necessary that some dendrites fall back behind the front and that others adjust by subsequent branching. To decrease λ_1, new primary dendrites can only be created from the array by development of tertiary dendrite arms. There is consequently an inherent hysteresis to adjustments of the primary spacing. Fig. 6, from Jackson et al. shows this very clearly. A' - velocity increase, B' - decrease to the original.

How, exactly, the reduced velocity causes side arm detachment is complex. The remelting can be caused by (a) a rise in temperature and (b), a rise in concentration of the interdendritic liquid. Analysis of array growth (18) under steady state conditions, indicates that the preferred stable conditions are when there is a limited interaction of solute rejection from adjacent dendrites ($\lambda_1, <\infty$), such that the undercooling is not at a minimum. A small reduction in velocity at constant spacing, is attended by a small reduction in tip undercooling (i.e. a temperature rise at the front), although the instant increase in tip radius, r_1, must simultaneously increase solute concentration between the dendrites, which are then "too close" for preferred stable array growth.

Therefore, although the analysis is complicated, this has to contain the explanation for there being so many detached dendrite fragments available in a typical columnar mushy region. "Typical", in the sense that the growth conditions are always transient, with V and G decreasing.

As noted elsewhere (16), the number of side arms in a dendritic array is enormous, eg. 10^6 - 10^7 cm^{-3}, so that even if only a minor fraction were to become detached, the number of fragments, potentially available, is more than adequate to promote intrinsic nucleation - if they can escape from the mushy zone.

The effects of liquid reentrainment by convection are probably of minor or negligible impor-

discounted, certainly for metals,
arms could only bend, but not

nment of the warmer liquid, is
also less concentrated than the
. solid will be deposited (prefer-
erated. This then is not an obvi-

growth conditions are transient -
falling continuously. It is neces-
nd it, respond to these changes.
wth rate, without convection, a
ackson et al. showed this effect
further at that time.

f curvature, r_1, responds imme-
eases, according to Vr_1^2 = con-
ot change rapidly, because it is
by the small anisotropy of the
, nor, with acceleration, does it
e dendrites fall back behind the
rease λ_1, new primary dendrites
y dendrite arms. There is conse-
spacing. Fig. 6, from Jackson et
e to the original.

nent is complex. The remelting
ncentration of the interdendritic
nditions, indicates that the pre-
n of solute rejection from adja-
minimum. A small reduction in
in tip undercooling (i.e. a tem-
radius, r_1, must simultaneously
re then "too close" for preferred

ontain the explanation for there
ypical columnar mushy region.
ways transient, with V and G

itic array is enormous, eg. 10^6 -
e detached, the number of frag-
te intrinsic nucleation - if they

ly of minor or negligible impor-

Fig. 6 Showing dendritic array growth in CBr_4, from Jackson et al (12), with acceleration at level A' and deceleration at level B', illustrating the rapid changes in tip radius, r_1, slower adjustment of primary spacing, λ_1, and detachment following deceleration.

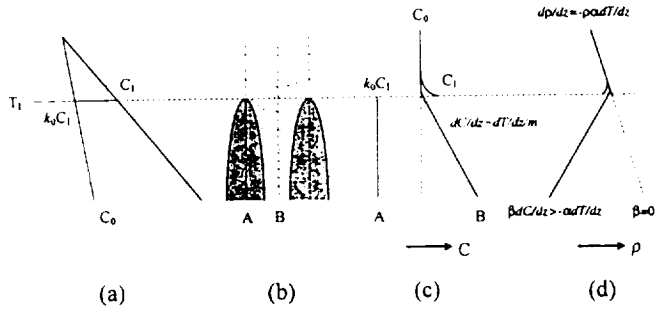

Fig. 7 The situation leading to thermo-solutal convection. Schematic plots for alloy of concentration, C_0, on phase diagram (a), with dendrite tip concentration, C_I, growing at an array front, (b), where the concentration vs height along axes A and B are as in (c) and the vertical liquid density profile is as in (d).

tance in this respect, but are all important for subsequent transport of the fragments, once they have become detached.

FRAGMENT TRANSPORT - HEAT PUMPS

The concern is with how detached dendrite arms can be transported from the mushy region of a casting into the bulk open liquid, where survivors may grow into new grains.

This is possible if interdendritic liquid, richer in solute, is less dense than the bulk liquid, despite being cooler, and occurs by thermo-solutal convection. The situation is most clearly demonstrated by solidification, vertically upwards, in a base chilled configuration, and becomes probable when the solutal density coefficient, β, is negative, and $\beta\Delta C$ exceeds $\alpha\Delta T$, where ΔC is the composition difference between an element of interdendritic liquid and the bulk, α is the coefficient of thermal expansion and ΔT the temperature difference corresponding to ΔC. From the phase diagram, $\Delta T/\Delta C = m_L$, the slope of the liquidus boundary.

There is then density inversion, given by $\Delta\rho = \rho(\beta\Delta C + \alpha\Delta T)$, between the interdendritic liquid at any position, with respect to the bulk liquid, and also between the solute boundary layer at the dendritic front and the latter, Fig. 7. Two convective regimes develope. First, at very short times, e.g. $\lesssim$ 10s, short range (< 10mm) oscillatory patterns form, close to the growth front. With growth vertically upwards, these create a mixing zone, immediately above the growth front, but the interdendritic liquid is not disturbed to any depth greater than that of the primary interdendritic spacing, λ_1 (typically $\approx$ 0.2mm). At longer times, eg. $\gtrsim 10^3$s, longer range channel plumes develope, of diameters $\approx$ 1 mm (3-5 primary dendrite spacings) and rise far (> 100mm) into the supernatant open liquid, Fig. 8. These are fed by lateral reentrainment of the warmer bulk liquid, which is drawn down through the dendritic mesh, cooled and recirculated into a wider interdendritic channel. Such channels are subsequently choked by smaller crystals and give rise to "freckel" defects in directionally solidified ingots (22). The channels are also richer in solute and are recognized in steel billet castings as "A" segregates.

It follows, in all of this, that the prime requirement for such developments depends upon there being a sufficiently large, negative solutal density coefficient, β, so that this form of thermosolutal convection is found in steels with carbon, silicon etc., or nickel base alloys containing aluminium or titanium, but is not to be expected in aluminium or magnesium alloys which are solidifying upwards, in which a majority of solutes (eg copper) are the more dense. This is why intrinsic nucleation is not found in such systems, as in D.C. castings, and why it is then necessary to use deliberate additions of heterogeneous substrates to promote equiaxed grains in foundry practice with these light metals.

Returning to the channel convection, it will be evident that the region in the mushy zone, below a convection plume is responsible for the near steady-state recirculation and behaves like a pump. The density inversion follows from the phase transformation which is driven by heat abstraction, so that the system behaves like a local heat pump. The relatively long range plumes also recirculate heat and solute into the open liquid, assisting in the heat transfer and causing macrosegregation. Typically, the rapid local convection translates about 1-2% of the liquid volume upwards while the balance sinks slowly. The macrosegregation above the dendritic front is described by an effective partition coefficient, $k_{eff} \gtrsim 0.9$ (23).

To analyze such a channel plume, as in Fig. 8, a simplified model can be used, supposing that a thin walled tube is inserted to some depth into the mushy region, h_D, and extends upwards

ransport of the fragments, once

PUMPS

nsported from the mushy region
grow into new grains.

less dense than the bulk liquid,
on. The situation is most clearly
base chilled configuration, and
negative, and $\beta\Delta C$ exceeds $\alpha\Delta T$,
t of interdendritic liquid and the
ie temperature difference corre-
slope of the liquidus boundary.

), between the interdendritic liq-
so between the solute boundary
ctive regimes develope. First, at
itory patterns form, close to the
ite a mixing zone, immediately
sturbed to any depth greater than
y ≈ 0.2mm). At longer times,
ieters ≈ 1 mm (3-5 primary den-
open liquid, Fig. 8. These are fed
is drawn down through the den-
ritic channel. Such channels are
"freckel" defects in directionally
and are recognized in steel billet

ich developments depends upon
efficient, β, so that this form of
ilicon etc., or nickel base alloys
ted in aluminium or magnesium
f solutes (eg copper) are the more
systems, as in D.C. castings, and
rogeneous substrates to promote

it the region in the mushy zone,
y-state recirculation and behaves
ransformation which is driven by
pump. The relatively long range
assisting in the heat transfer and
tion translates about 1-2% of the
macrosegregation above the den-
$k_{eff} \geq 0.9$ (23).

nodel can be used, supposing that
region, h_D, and extends upwards

into the open liquid, to some height h_L. The resulting recirculation becomes a fountain - a salt fountain (24) - driven by the pressure difference, $P = \Delta\rho\, g h_D$, at its base.

Flow is essentially streamlined, in the channel-plume pipe and also through the mesh, downwards - estimates of Reynolds numbers confirm this (25). The volume of liquid flowing upwards, $V\uparrow = \pi P.r^4/8h_L\eta$, must equal that flowing downwards, $V\downarrow$, to supply liquid around the edge of the base of the pipe, of circumference $2\pi r$. Description of the flow channel paths, through the dendritic mesh is a more complicated problem, depending on its permeability and hence, upon the primary and secondary dendrite arm spacings, λ_1 and λ_2, and the fraction of solid, f_s. The pressure difference, P, at the base of the pipe is the same for upward and downward flow. Therefore, for a given system and set of growth conditions, it must follow that

$$C_1 r^4\uparrow = C_2 r\downarrow$$

where C_1 and C_2 are constants and $r = (C_2/C_1)^{1/3}$.

The viscosity is essentially constant, so that for any r, the volume flow rate through the fountain is dictated by the permeability of the mushy region down to the depth, h_D. This, in turn, is dependent on the primary and secondary dendrite spacing, λ_1, which is itself related to D_L/V_d, the solute diffusion coefficient and dendritic growth rate. Since liquid diffusion rates are generally well within an order of magnitude (around $10^{-9}m^2s^{-1}$) it becomes understandable why channel plume dimensions (although not the flow rates in them) are so similar from system to system, metallic, aqueous, organic.

It is possible to make artificial salt fountains of this type, where the radius, r, and lengths, $(h_L + h_D)$, are predetermined, but in the unconstrained natural setting, the model is relaxed and the situation becomes more involved.

The basic balance remains, i.e. the upward and downward flows must remain equal, so that r is still of the form, $(C_2/C_1)^{1/3}$, but solutions to C_1 and C_2 are more difficult: We suppose that the effective pressure term remains the same for upward and downward flows, but the walls of the channel within the mushy region are now permeable and receive recirculating liquid over a depth range, so that h_D is no longer precisely defined, - there is a continuum of possible entrainment paths, through the dendritic array. At the same time, there is no stationary rigid wall to the plume, pipe, because the surrounding liquid is drawn up with it. The essential requirement for this type of flow is that although thermal equilibrium is approached rapidly (between the cooler liquid of the mushy zone and that of the supernatant bulk), solute diffusion is so much slower, that the plume composition remains essentially constant for long times (and therefore distances). The composition profile across a plume is therefore of a square wave form, while the velocity profile is smeared out over several plume diameters. Such a profile can be described by spline fitting a parabolic velocity profile for the plume core, with an exponential profile for the surroundings - Fig. (9). Analysis of such plume flow shows that in transparent systems (aqueous, organic) the observed flow rates can be related to the buoyancy forces satisfactorily, and, by extrapolation, can be used to predict plume flow rates in opaque metals. Although plume dimensions are very similar, cf. above, flow rates within them are in a ratio, metallic: aqueous: organic ≈ 100:10:1 mms^{-1}, reflecting, primarily, the respective thermal conductivities and kinematic viscosities (22) as in the Pécklet numbers. The above mentioned "constant", C_1, is then to some extent numerically soluble and supported by experimental measurement, but the reentrainment is the more difficult to describe. Part of this latter problem arises because the fraction of solid in the upper part of

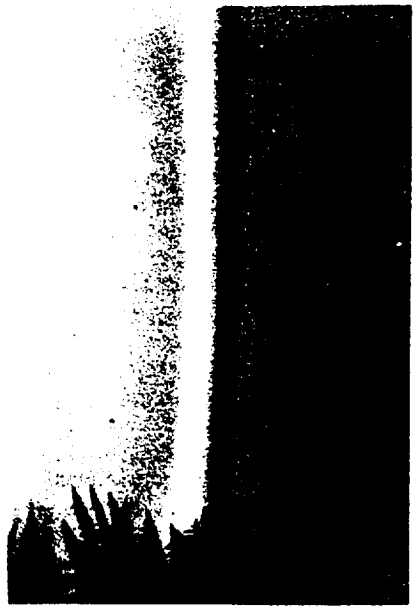

Fig. 8. Showing convection plume above dendritic growth front of NH_4Cl-H_2O, from (22), solute contrast of refractive index, plume width $\lesssim$ 1 mm.

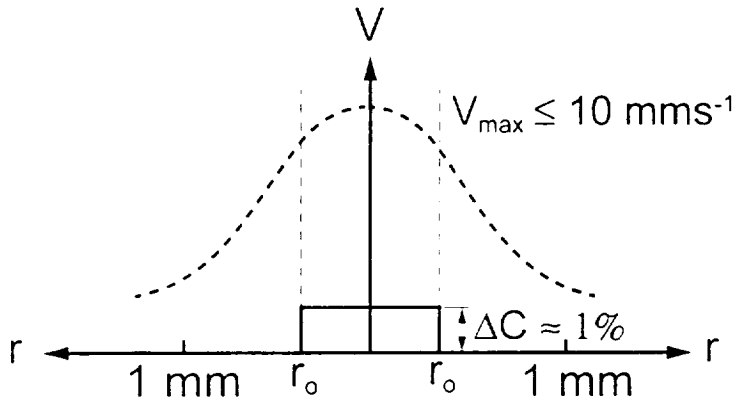

Fig. 9 Schematic velocity profile, V, and step concentration difference, ΔC, across a plume as in Fig. 8.

dendritic growth front of
st of refractive index, plume

nax ≤ 10 mms^{-1}

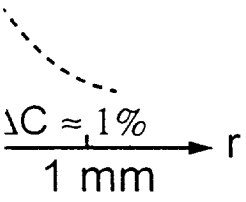

:p concentration difference,

the mushy region is quite small (eg < 10%), so that fluid flow through the mesh does not take place along identifiable, discrete channels, but rather around a very permeable array of primary and secondary cylindrical obstacles (somewhat similar to water flowing through a reed bed). The shortest paths for reentrainment are obviously near the channel mouth, which is where the cone of primary dendrites surround the cooler plume liquid. At some lower depth, $\lesssim$ 5 - 10mm, the interdendritic liquid is essentially quiescent, and the width of the pump activity is not more then about twice this depth - hence the typical plume spacing.

The result of these relaxations (on the rigid pipe model) is to increase the flow rate in a channel plume - by making the base of the pipe more open and by removing the constraint of rigid walls. Observation and calculations for the NH_4Cl-H_2O system, indicate an increase in flow rate by a factor of about x 5 (see appendix B, ref. 22). Description of the interdendritic flow pattern and rates remains empirical, at present, and this complicates analysis of side arm transport from the mushy zone see, e.g. Poirier et al (26, 27) and Beckermann et al (28-30).

SUMMARY - CONCLUSIONS

- Without thermosolutal convention to transport dendrite fragments from the mushy zone of a casting into open liquid, nucleation of equiaxed grains is generally promoted by addition of grain refining substrates. The grain size can then be modelled by time dependent, heterogeneous nucleation, although description of the substrate efficiency remains obscure and requires arbitrary assumptions.

- With density inversion in the columnar mushy zone, thermo-solutal convection provides a mechanism to disperse dendrite fragments into the melt and equiaxed grain formation/ nucleation can be intrinsic, subject to fragment survival in the melt.

- The detachment of dendrite side arms in the mushy region is accelerated by temperature rise and by solute enrichment of interdendritic liquid. This situation is promoted by the typically decreasing growth rates and temperature gradients at the columnar growth front of a casting, and occurs because the primary dendrite spacing does not automatically adjust to the continuously changing conditions, while the dendrite tip radius does so, immediately and continuously.

- In a vertical configuration, finger and plume convention patterns develop if solute is sufficiently less dense than solvent, and thus offers a mechanism for efficient dispersion of crystal fragments into the melt. This mechanism is not generally available in light metals, especially in vertical configurations.

- Analysis of plume convection allows flow rates and dimensions to be predicted with some confidence, describing the mechanism in terms of a heat pump. The most intractable part of such modelling remains in analysis of interdendritic flow patterns.

ACKNOWLEDGEMENTS

This paper is based on experimental observations and calculations by Shu Zu Lu, George Hansen and Scott Steube at Michigan Technological University, being part of a program supported by the National Science Foundation, through the Division of Materials Research, Metallurgy Program, NSF-DMR-9206783 and the National Aeronautics and Space Administration, Micro-gravity Program, through NASA-Lewis Research Center, NAG-3-1659.

REFERENCES

1. M. Rappaz and Ch.-A. Gandin, Acta Met & Mat., 41 (1993), 345-360.
2. D.D. Goettsch & J.A. Dantzig, Metall. Trans., 25A (1994), 1063-1079.
3. Ch. Charbon, A. Jacot and M. Rappaz, Acta Met & Mat., 42 (1994), 3953-3966.
4. W. Oldfield, Trans. ASM., 59 (1966), 945-958.
5. E.L. Glasson and E.F. Emley, The Solidification of Metals, The Iron and Steel Soc., Book No. 110 (1968) 1-9.
6. A. Hellawell, The Solidification and Casting of Metals, The Metals Society, Book No. 192 (1979), 161-168.
7. I. Maxwell and A. Hellawell, Acta Met., 23 (1975), 229-237.
8. I.G. Davies, J.M. Dennis and A. Hellawell, Metall. Trans., 1A (1970), 275-282.
9. L. Backerud, Jernkontorets Ann., 155(8), (1971), 422-430.
10. I. Maxwell and A. Hellawell, Acta Met., 23 (1975), 895-901.
11. G.J. Davies, Solidification and Casting, Applied Science Pub. Co. (London), Chapter 6 (1973).
12. K.A. Jackson, J.D. Hunt, D.R. Uhlmann and T.P. Seward, Trans. TMS - AIME, 236 (1966), 149-160.
13. T.F. Bower and M.C. Flemings, Trans. TMS-AIME, 239 (1967), 1620-1627.
14. M.E. Glicksman and R.J. Schaefer, The Solidification of Metals, Iron and Steel Soc., Book No. 110, (1967), 43-48.
15. C.Y. Wang and C. Beckerman, Metall. Trans., 25A (1994), 1081-1093.
16. G. Hansen, A. Hellawell, S.Z. Lu and R.S. Steube, TMS Fall Meeting, 1994, Rosemont, Illinois, Metall. Trans., to be published.
17. D.J. Fisher and W. Kurz, Principles of Solidification, Trans. Tech Publications (1994), Chapter 4.
18. J.D. Hunt and S.Z. Lu, T.M.S. Fall Meeting, 1994, Rosemont, Illinois, Metall. Trans., to be published.
19. H. Muller-Krumbhaar and W. Kurz, Materials and Technology: A Comprehensive Treatment, Eds. Cahn, Haasen and Kramer, VCH (New York), 5 (1991), 553-562.
20. M.E. Glicksman, TMS Fall Meeting, 1994, Rosemont, Illinois, Metall. Trans., to be published.
21. R.S. Steube and A. Hellawell, Video Journal of Engr. Research, 3 (1993), 1-16.
22. A. Hellawell, J.R. Sarazin and R.S. Steube, Phil. Trans. Roy. Soc. (London), 345A (1993), 507-544.
23. J.R. Sarazin and A. Hellawell, Metall. Trans., 19A (1988), 1861-1871.
24. M.E. Stern, J. Fluid Mechanics, 35 (1969), 209-230.
25. A.K. Sample and A. Hellawell, Metall. Trans., 15A (1984), 2163-2173.
26. G. Ganesan and D.R. Poirier, Metall. Trans., 21B (1990), 173-181.
27. S.D. Felicelli, J.C. Henrich and D.R. Poirier, Metall. Trans., 22B (1991), 847-859.
28. J. Ni and C. Beckermann, Metall. Trans., 22B (1991), 349-357.
29. H.C. deGroh III, P.D. Weidmen, R. Zakhem, S. Ahuja and C. Beckermann, Metall. Trans., 24B (1993), 749-753.
30. C.Y. Wang, S. Ahuja, C. Beckermann and H.C. deGroh III, Metall. Trans., 25B (1994), 1-9.